RNA (1999), *5*:102–116. Cambridge University Press. Printed in the USA.

Guanosine 2-NH_2 groups of *Escherichia coli* RNase P RNA involved in intramolecular tertiary contacts and direct interactions with tRNA

CORINNA HEIDE,[1] THOMAS PFEIFFER,[1] JAMES M. NOLAN,[2] and ROLAND K. HARTMANN[1]

[1]Medizinische Universität zu Lübeck, Institut für Biochemie, Ratzeburger Allee 160, D-23538 Lübeck, Germany
[2]Department of Biochemistry SL43, Tulane University Medical Center, 1430 Tulane Avenue, New Orleans, LA 70112-2699, USA

ABSTRACT

We have identified by nucleotide analog interference mapping (NAIM) exocyclic NH_2 groups of guanosines in RNase P RNA from *Escherichia coli* that are important for tRNA binding. The majority of affected guanosines represent phylogenetically conserved nucleotides. Several sites of interference could be assigned to direct contacts with the tRNA moiety, whereas others were interpreted as reflecting indirect effects on tRNA binding due to the disruption of tertiary contacts within the catalytic RNA. Our results support the involvement of the 2-NH_2 groups of G292/G293 in pairing with C_{74} and C_{75} of tRNA CCA-termini, as well as formation of two consecutive base triples involving C_{75} and A_{76} of CCA-ends interacting with G292/A258 and G291/G259, respectively. Moreover, we present first biochemical evidence for two tertiary contacts (L18/P8 and L8/P4) within the catalytic RNA, whose formation has been postulated previously on the basis of phylogenetic comparative analyses. The tRNA binding interference data obtained in this and our previous studies are consistent with the formation of a consecutive nucleotide triple and quadruple between the tetraloop L18 and helix P8. Formation of the nucleotide triple (G316 and A94:U104 in wild-type *E. coli* RNase P RNA) is also supported by mutational analysis. For the mutant RNase P RNA carrying a G94:C104 double mutation, an additional G316-to-A mutation resulted in a restoration of binding affinity for mature and precursor tRNA.

Keywords: gel retardation; inosine interference; mutations in loop L18 and helix P8; nucleotide analog interference mapping (NAIM)

INTRODUCTION

Ribonuclease P (RNase P) is the ubiquitous processing enzyme that generates the mature 5′-termini of tRNAs. It is a ribonucleoprotein in vivo, with the exception of RNase P from spinach chloroplasts, whose composition was reported to be purely proteinaceous (Wang et al., 1988). In vitro, RNA subunits of RNase P enzymes from Bacteria are catalytically active in the absence of the protein component (Guerrier-Takada et al., 1983). They are the only known RNA catalysts naturally devoted to act *in trans*.

RNase P enzymes recognize the acceptor stem/T arm modules of tRNA molecules (e.g., McClain et al., 1987; Forster & Altman, 1990a; Kahle et al., 1990; Thurlow et al., 1991; Schlegl et al., 1992; Hardt et al., 1993a; Carrara et al., 1995; Yuan & Altman, 1995). Substrate recognition has been studied most extensively for bacterial RNase P enzymes. Binding of tRNA to the catalytic RNA mainly relies on tertiary contacts between functional groups of the two RNA molecules. One region of Watson–Crick-type base-pairing, involving the two consecutive cytosines of tRNA CCA-termini and two guanosines in the internal L15/16 loop of *Escherichia coli*-like "type A" (Haas et al., 1996) RNase P RNAs, has been indicated by genetic studies (Kirsebom & Svärd, 1994). Five functional groups in the T stem-loop of yeast $tRNA^{Phe}$, including four ribose 2′-hydroxyls and the 4-amino group of the conserved C56, were shown to be crucial for binding to *Bacillus subtilis* RNase P RNA (Loria & Pan, 1997). Biochemical, mutational, and photoaffinity crosslinking data indicate that the P7–P11 region of bacterial RNase P RNA is the main interaction site for the T stem-loop of tRNAs (Nolan et al., 1993; Harris et al., 1994; Pan et al., 1995; Loria & Pan, 1997). The 2′-hydroxyl of

Reprint requests to: Roland K. Hartmann, Medizinische Universität zu Lübeck, Institut für Biochemie, Ratzeburger Allee 160, D-23538 Lübeck, Germany; e-mail: hartmann@biochem.mu-luebeck.de.

tRNA nucleotide 62 was inferred to interact with A230 of *B. subtilis* RNase P RNA (Pan et al., 1995). Binding interference studies have identified *pro*-Rp oxygens and 2′-OH groups in *E. coli* RNase P RNA whose modification impairs tRNA binding (Hardt et al., 1995b, 1996). A subset of these functional groups are potential candidates for direct contacts to the tRNA moiety, particularly those residing in regions reported to form photoreactive crosslinks with tRNA molecules. Another subset of interfering modifications is anticipated to affect tRNA binding indirectly by perturbing crucial tertiary interactions or by favoring alternative folding states. Since the gel retardation assay applied in this and previous studies (Hardt et al., 1995b, 1996) selects for thermodynamically stable tRNA binding to *E. coli* RNase P RNA under moderate salt conditions (0.1 M NH_4^+, 0.1 M Mg^{2+}), it is considered to be a sensitive probe for the detection of functional groups involved in tRNA binding either directly or indirectly. Of course, one cannot exclude that some of the information obtained here may not be equally valid for every functional state of RNase P RNA, since the catalytic RNA may undergo conformational changes during the catalytic cycle, and different substrates and products may bind in a nonidentical fashion (Guerrier-Takada & Altman, 1993; Kufel & Kirsebom, 1996a; Pan & Jakacka, 1996; Westhof et al., 1996).

Here we have extended the tRNA binding interference approach to inosine modifications to identify exocyclic NH_2 groups of guanosines in RNase P RNA from *E. coli* that are important for tRNA binding. The majority of observed interference effects were at conserved G residues. In this study we were able to assign a subset of interference effects to direct interactions between RNase P RNA and tRNA, whereas others are attributable to indirect effects by virtue of disturbing the integrity of tertiary structural elements within the catalytic RNA. Our results provide direct biochemical evidence for the base-pairing of G292/G293 to the 3′-terminal C residues of tRNAs, as inferred from mutational studies (Kirsebom & Svärd, 1994). We further present results supporting the formation of two consecutive base triples involving C_{75} and A_{76} of tRNA CCA-termini that interact with G292/A258 and G291/G259 of *E. coli* RNase P RNA, as recently proposed by Easterwood & Harvey (1997), and data in support of two tertiary contacts, one between G316/A317 in L18 and two consecutive base pairs in P8 (Brown et al., 1996), and another involving A99 in L8 and base pair C71:G356 in P4 (Massire et al., 1998). Additional support for the L18-P8 interaction is provided by mutational analysis of the nucleotide triple (G316 and A94:U104 in wild-type *E. coli* RNase P RNA): mutant RNase P RNA carrying the G94:C104 double mutation in helix P8 regained substantial binding affinity for mature as well as precursor tRNA after a G-to-A exchange at position 316.

RESULTS

Nucleotide analog interference mapping (NAIM)

NAIM approaches exploit the potential of phosphorothioate-specific cleavage of nucleic acids by iodine (Gish & Eckstein, 1988). In this study, a pool of *E. coli* RNase P RNAs carrying randomly distributed inosine Rp-phosphorothioate modifications (IMPαS, Fig. 1) was analyzed for tRNA binding. It has been documented previously that Sp-NTPαS analogs are incorporated with essentially the same efficiency as normal NTP substrates by T7 RNA polymerase (Christian & Yarus, 1992). We also observed very similar efficiencies of GTPαS and ITPαS incorporation by T7 RNA polymerase, and inosines are accurately incorporated in place of guanosines (Strobel & Shetty, 1997). A low level of IMPαS modification (2.5%) was chosen to minimize the probability that RNAs carry more than one modification per molecule at functionally important locations, which may mask weaker interference effects (Christian & Yarus, 1992). Partially modified RNase P RNA pools were separated into tRNA-binding and nonbinding fractions by gel retardation and then subjected to iodine cleavage (Hardt et al., 1995b, 1996; see Materials and Methods). Interference effects are observed at those positions where the iodine hydrolysis product is diminished in the tRNA-binding RNase P RNA fraction but enhanced in the nonbinding fraction. A comparison of interference patterns obtained for Rp-IMPαS- and Rp-GMPαS-modified RNase P RNA pools allowed us to distinguish between effects attributable to the phosphorothioate and/or the inosine modification. This approach has the

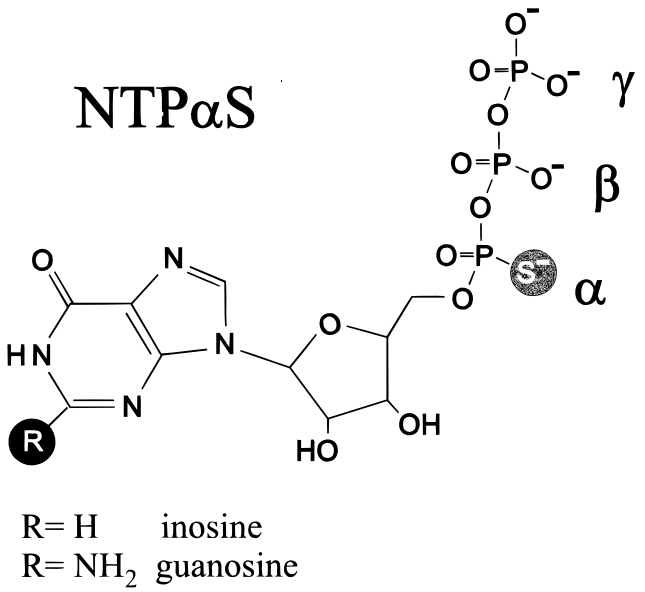

FIGURE 1. Illustration of guanosine and inosine 5′-α-thiotriphosphate (Sp-diastereomer) analogs used in T7 transcriptions of *E. coli* RNase P RNA.

inherent limitation that strong interference effects due to the phosphorothioate modification per se are insensitive to the testing of the additional modification.

Sites of inosine interference

Comparative iodine hydrolysis patterns of the two functionally separated *E. coli* RNase P RNA fractions, originating either from partially GMPαS- or IMPαS-modified RNase P RNA pools, are shown in Fig. 2A for the region of nt 270 to 332. Only sites of interference reproducibly detected in three to six independent experiments are depicted by circles. For example, interference effects at nt 291–293 were observed with IMPαS but not GMPαS, and are thus entirely attributable to the inosine modification. Combined effects were found at G300 and G316. Here, phosphorothioate interferences are enhanced by the additional inosine modification. Other examples of interfering positions are illustrated in Figure 2B. All found sites of inosine interference are summarized within the secondary structure model (Fig. 3) and have been classified according to their relative strength (Table 1). Strong interference ($>$50%) with gel-resolvable tRNA^{Gly}(intron) binding was observed for IMPαS but not GMPαS substitutions at guanosines 19, 63, 230, 291–293, 306, 329, and 356. Moderate interference effects (25–50%) solely due to the inosine modification were located at G64, 95, 137, 304, and 314, and weak effects ($<$25%) to G22, 30, and 105–109. We cannot draw any conclusion with regard to the inosine modification at G68 because of an essentially complete phosphorothioate effect at this position. At several positions we have observed weak or moderate interference effects for the GMPαS modification alone, which were enhanced in the presence of the IMPαS double modification. At these locations, both the sulfur substitution at the 5′-phosphate and the absence of the exocyclic amino group contributed to a weakening of tRNA binding. This pertains to G72, G250/251, G300, G316, and possibly G259–262 (Table 1). Phosphorothioate interference effects at G250/251, G259–262, and G316 were not detected in our previous study (Hardt et al., 1995b), which we attribute to the fact that the present study included the analysis of 3′- in addition to 5′-end-labeled RNase P RNA and a more rigorous quantification of interference effects. Inosine interference at G259–262 (Fig. 2B) and G105–109 (not shown) could not be assigned to individual G residues because of unsatisfactory gel resolution (Fig. 2B). G250/251 represented a similar case, although the main interference effect appeared to be at G250.

The P8 and L18 regions—sites of interference and mutational analysis

Analysis of an enlarged collection of bacterial RNase P RNAs revealed that in the majority of RNAs a G at position 316 covaries with an A:U pair at position 94:104, while an A at position 316 covaries with a G:C pair at this location (Brown et al., 1996). This finding led to the conclusion that the tetraloop L18 interacts with helix P8, probably comprising nt 316 and 317 in L18 and the consecutive base pairs at position 94:104 and 95:103 in helix P8. However, attempts to provide experimental support for the proposed tertiary interaction had been unsuccessful (Brown et al., 1996). The molecular basis of the L18-P8 tertiary interaction was proposed to involve two consecutive nucleoside triples of the type reported by Jaeger et al. (1994) in the context of a mutational study of the *Tetrahymena* group I intron.

We have observed a variety of nucleotides in the L18 and P8 regions in this and our previous studies (Hardt et al., 1995b, 1996) at which Rp-phosphorothioate-, 2′-deoxy-, and/or inosine modifications interfered with tRNA binding (summarized in Fig. 4A). Interference effects may either reflect a perturbation of direct contacts to the tRNA or may affect tRNA binding indirectly by disrupting RNase P RNA structure. Based on the phylogenetic evidence mentioned above (Brown et al., 1996), interference effects observed in the L18 and P8 regions are likely to reflect an indirect effect on tRNA binding by means of perturbing the L18-P8 tetraloop-helix interaction. This is also in line with the finding that helix P8 is part of the four-helix junction that is thought to be the main interaction site for the T arm of tRNA molecules (Nolan et al., 1993; Harris et al., 1994; Pan et al., 1995; Loria & Pan, 1997).

Figure 4B,C summarizes a model of the L18-P8 interaction based on the proposed nucleoside triple structures of Jaeger et al. (1994), but with the modifications outlined below. First, we incorporated an additional interaction involving the tetraloop nucleotides G314 and A317 (Fig. 4B) for the following reasons: (a) this type of interaction between the first- and last-loop nucleotide has recently been observed in two GNRA tetraloop-helix contacts in crystal structures of the hammerhead ribozyme and the P4/P6 domain of the *Tetrahymena* ribozyme (Pley et al., 1994; Cate et al., 1996), and (b) this type of interaction is fully supported by our interference data (Fig. 4A). Second, we propose hydrogen bonding between the 2-NH_2 group of G316 and O2 of U104 to account for the observed inosine interference effect at G316 (Fig. 4A,C). The nucleotide quadruple and triple shown in Figure 4B,C would be supported by inosine interference effects at G95, 314, and 316, as well as by Rp-phosphorothioate interference at A317 (Fig. 4A). However, the triple nt 316/94:104 in Figure 4C predicts a 2′-deoxy interference effect at A94, which we have not observed.

An alternative model of the L18-P8 interaction (Fig. 4D,E) is consistent with the bulk of our interference data. While the triple is a model proposed by analogy to an A/G:C triple seen in the crystal structure of the hammerhead ribozyme (Pley et al., 1994), this

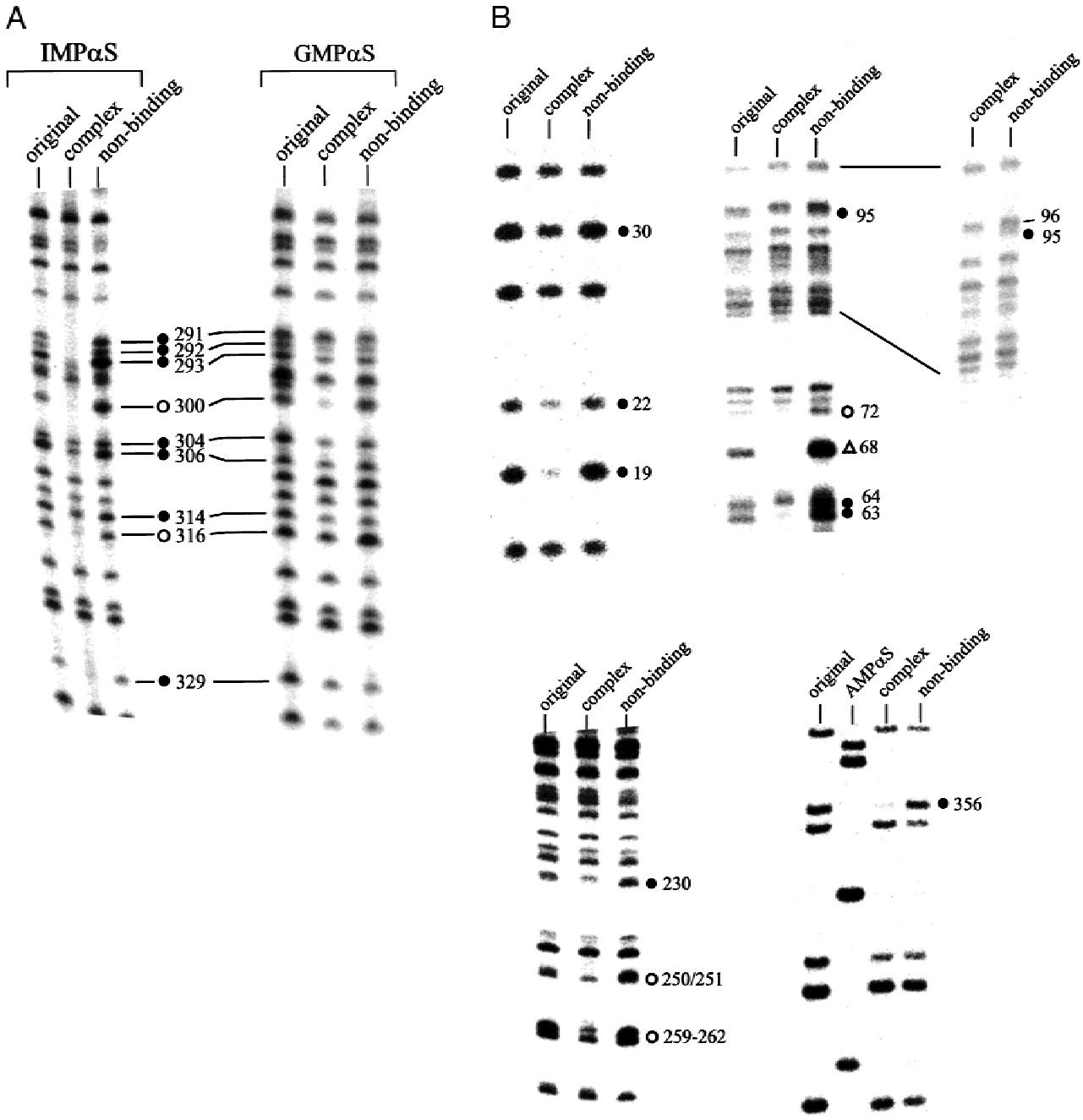

FIGURE 2. Iodine cleavage analysis of tRNA binding interference experiments. Partially Rp-IMPαS-modified 5′-^{32}P-labeled *E. coli* RNase P RNAs were selected for $tRNA^{Gly}_{(intron)}$ binding under conditions of 1 × buffer A (see Materials and Methods); original: the original partially modified RNase P RNA pool; complex: RNase P RNA fractions recovered from the complex with $tRNA^{Gly}_{(intron)}$; non-binding: RNase P RNA fractions that did not bind to $tRNA^{Gly}_{(intron)}$. **A:** Comparative Rp-IMPαS and Rp-GMPαS hydrolysis patterns are shown exemplarily for sites of interference between nt 270 and 332. **B**: Illustration of other sites of inosine interference. A sequence ladder generated by iodine hydrolysis of Rp-AMPαS-modified RNase P RNA was included for the analysis of the 3′-P4 region (G356). Nucleotide positions indicated by circles are sites of tRNA binding interference effects attributable to the inosine modification alone (black circles) or to both the Rp-phosphorothioate and the inosine modification (open circles); the triangle (G68) indicates a 100% Rp-phosphorothioate interference effect. Interference effects were verified in three to six independent experiments. Also, to compensate for fluctuations in the amount of material loaded on gels, corresponding hydrolysis bands in the tRNA-binding (complex) and nonbinding RNase P RNA lanes were normalized to the average intensity differences of three to four reference bands for which an interference effect was absent (see Materials and Methods). Gel resolution and thus assignment of interference effects was poor for G105–109 (not shown), G250/251 and G259–262. However, in the latter two cases, interference effects appeared to be predominantly at G250 and G259/260. A second example of the G95 region is included to illustrate that the site of interference is at G95 rather than G96.

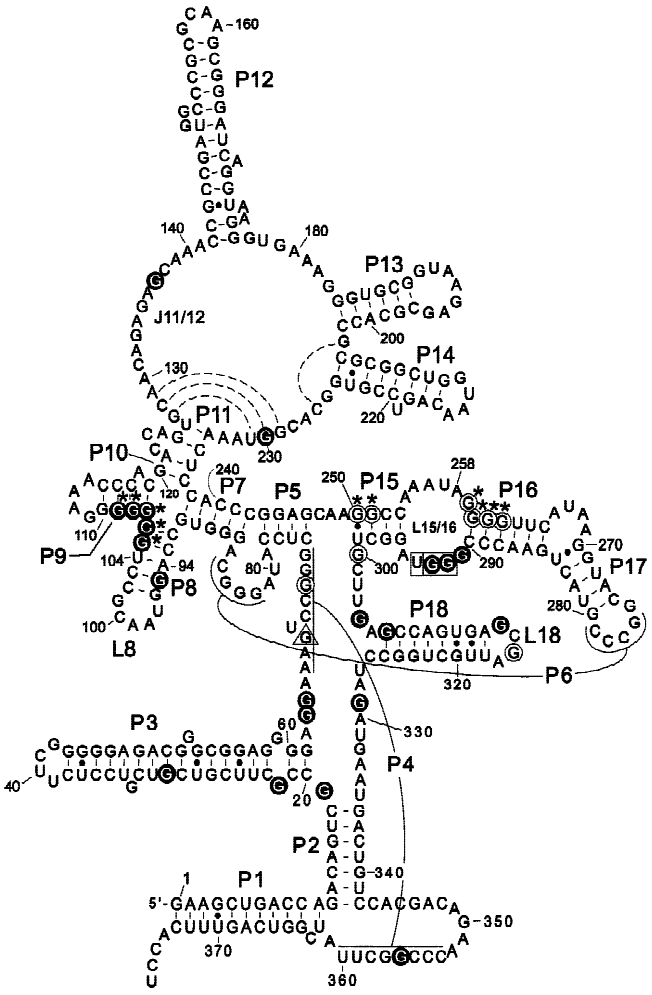

FIGURE 3. Secondary structure of wild-type *E. coli* RNase P RNA according to Haas et al. (1994), Mattsson et al. (1994) and Massire et al. (1998). P: helical regions; L: loop regions; J: joining segments named according to the numbers of helices they connect. Nucleotides at which an Rp-IMPαS double modification, but not the Rp-GMPαS modification alone, interfered with tRNA binding are indicated by black circles and white letters; positions where interference effects were enhanced for the Rp-IMPαS compared with the Rp-GMPαS modification are marked by open circles; circled nucleotides marked by asterisks: because of limited gel resolution, individual contributions to observed interference effects of guanosines at positions G105–109, G250/251 and G259–262 could not be assigned unequivocally. However, for the latter two regions, main effects appeared to be at G250 and G259/260 (Fig. 2B). The triangle (G68) indicates a 100% Rp-phosphorothioate interference effect. For the relative strength of interference effects see Table 1. RNase P RNAs carried an additional G (not shown) at the 5′ end for efficient transcription by T7 RNA polymerase. For RNase P RNAs transcribed from plasmid pSP64M1 linearized with *Bam*HI, the shown 3′ end was extended by GGAUC. In the case of RNase P RNA transcribed from plasmid pSP64M1HH (see Materials and Methods), 3′ ends derived from hammerhead self-cleavage had the sequence $_{370}$UUUCACGUC>p (mutation underlined). Boxed nucleotides G292-U294: sites of interaction with CCA of tRNA 3′-termini (grey-shaded; Kirsebom & Svärd, 1994) and extended interaction also involving the discriminator base of tRNA NCCA termini (open and grey-shaded boxes; Tallsjö et al., 1996).

type of quadruple has up to now been observed in crystal structures of the hammerhead ribozyme and the P4/P6 domain of the *Tetrahymena* group I intron (Pley et al., 1994; Cate et al., 1996), involving exactly the same hydrogen bonding interactions as shown in Figure 4D. The two crystallographic precedents now available lead us to favor the models shown in Figure 4D,E.

To gain further experimental support for the L18-P8 interaction, we analyzed several RNase P RNA variants with mutations in the two regions. A mutant with an inversed G:C pair at position 95:103 (Mut 0, Fig. 5) showed a minor (threefold) but reproducible decrease in tRNA binding affinity, which also holds true for the G316-to-A mutant (Mut 1). It should be noted that we always coelectrophoresed the wild-type RNase P RNA and the mutant RNA under investigation to compensate for fluctuations (temperature, current) in individual gel retardation experiments. In all independent experiments (three to six per mutant RNA), the mutant RNAs Mut 0 and Mut 1 showed weaker binding than the wild-type RNase P RNA. An A317-to-G mutation (Mut 2 and Mut 5) essentially abolished gel-resolvable tRNA binding (Fig. 5). Since RNA folding predictions suggested that this mutation may cause aberrant folding in the P18 region, we analyzed this mutant RNase P RNA by lead probing in comparison with wild-type RNase P RNA and variant Mut 1. Variant Mut 2 clearly showed increased susceptibility to lead hydrolysis in the P15-J15/18-P18 region (Fig. 6), supporting the suspicion that an A317-to-G exchange induces severe misfolding of RNase P RNA. This is consistent with the observation that all A-type (*E. coli*-like; Haas et al., 1996) bacterial RNase P RNAs carrying the P18 module possess an A at this location, except for one isolate (LGW#23; Brown, 1998; RNase P database). Variant Mut 3, carrying two double mutations (G94:C104 and A95:U103) in P8, showed reduced tRNA binding affinity (Fig. 5). However, an additional base exchange (G316 to A, Mut 4) resulted in a restoration of binding affinity. These results provide the first direct experimental evidence for a G316/A94:U104 or an A316/G94:C104 triple as part of the L18-P8 tertiary contact. The equal importance of this interaction for the binding of mature tRNA^{Gly} and precursor tRNA^{Gly} (Fig. 5) indicates that formation of this contact optimizes binding of the tRNA moiety.

DISCUSSION

The P15/P16 region

The strong inosine interference effects at G292 and G293 (Table 1) provide direct experimental evidence for the two exocyclic amino groups at G292/293 being involved in Watson–Crick base pairing with the two cytosines of tRNA $_{73}$NCCA$_{76}$ 3′-termini, as inferred from mutational studies (Kirsebom & Svärd, 1994; Svärd

TABLE 1. Quantification of (**A**) IMPαS and (**B**) combined GMPαS/IMPαS interference effects, using a Bio-Imaging Analyzer BAS-1000 (FUJIFILM) and the software PCBAS (Raytest).

A

position	IMPαS interference (%)
19	54
22	14
30	11
63	90
64	44
95	42
105-109	18
137	43
230	52
291	100
292	100
293	100
304	47
306	59
314	31
329	80
356	66

B

position	GMPαS+IMPαS interference (%)
68	100, 100
72	27, 76
250/251	26, 52
259-262	31, 34
300	69, 100
316	37, 72

IMPαS: grey-shaded bars; GMPαS: black bars. Each quantification was based on three to six independent experiments, and deviations between individual experiments were below ± 15%. To compensate for intensity fluctuations in iodine hydrolysis patterns of tRNA-binding and nonbinding RNase P RNA fractions, each position of interference was normalized to the average intensities of three to four reference bands for which an interference effect was not apparent (for details, see Materials and Methods). In the case of combined phosphorothioate and inosine interference effects, indicated interferences are cumulative: for example, the intensity of the iodine hydrolysis band at G300 was reduced by 69% in the tRNA-binding RNase P RNA fraction using GMPαS-modified RNase P RNA pools, but was reduced essentially to zero with the IMPαS double modification. G300 thus represents a borderline case, where the phosphorothioate modification per se almost masks the inosine effect under the conditions tested. Note that interference effects in the regions of G105–109 and G259–262 could not be assigned unambiguously to individual guanosines because of unsatisfactory gel resolution (see Fig. 2B). Thus, interference effects were quantified for the G clusters as a whole. The same pertains to G250/251, although the main interference effect could be assigned to G250 (Fig. 2B).

et al., 1996). The strong inosine interference at G291 is the first biochemical support for a bifurcate H-bonding interaction between the 2-NH_2 group of G291 and the N7 and O6 of G259, as proposed recently in a computer model of of the J15/16 bulge loop complexed with a tRNA ACCA 3′-terminus (Easterwood & Harvey, 1997). In the aforementioned model, G259, G291, and A_{76} of tRNA CC*A*-termini as well as G292, A258, and C_{75} of C<u>C</u>A form coplanar base triples stacked upon each other (Fig. 7). We also identified a c7-deaza modification at G292 that interferes with tRNA binding (unpubl. results). This observation is consistent with H-bonding involving N7 of G292 and the 6-NH_2 group of A258 (Fig. 7). Taken together, our results provide experimental support for several molecular details of the RNase P RNA-NCCA interaction as predicted in the Easterwood and Harvey model.

Further interference effects could be assigned to the region of nt 259–262 (Table 1). The four guanosines at this location, however, migrated as two bands on PAA/urea gels (Fig. 2B). We tentatively assigned one band to G259 and/or G260 and the second to G261 and/or G262. The interference of intermediate strength was essentially attributable to the Rp-phosphorothioate modification (Table 1). The iodine hydrolysis band assigned to G259/260 showed a stronger interference effect than the band assigned to G261/262 (Fig. 2B). G259 of *E. coli* RNase P RNA was shown to be protected from kethoxal modification (kethoxal modifies the N1 and N2 positions of guanosines) in the presence of (p)tRNA carrying an intact CCA terminus. Deletion of the terminal A_{76} of CCA abolished protection at this location (LaGrandeur et al., 1994) and A_{76} contributes to the high-affinity binding of (p)tRNA to RNase P RNA (Hardt

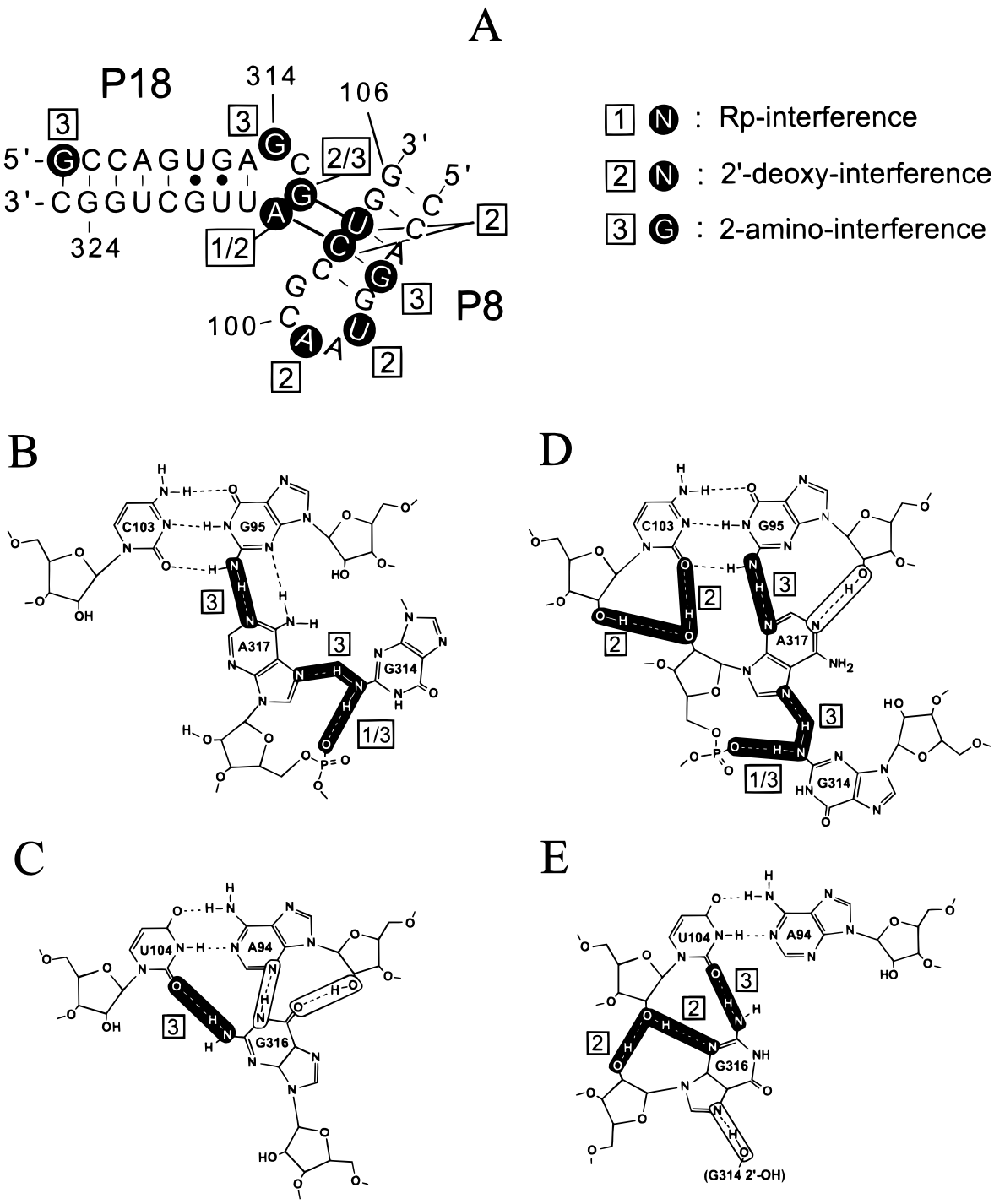

FIGURE 4. **A**: Observed modifications in P18 and P8 that interfere with tRNA binding to *E. coli* RNase P RNA (this study; Hardt et al., 1996). **B,C**: Proposed interaction between **B** G314/A317/G95:C103 and **C** G316/A94:U104 of *E. coli* RNase P RNA. The shown interactions are extended versions of nucleoside triples reported by Jaeger et al. (1994) in the context of a mutational study of the *Tetrahymena* ribozyme. **D,E**: Alternative models of the quadruple and triple. The base triple involving G316 is proposed by analogy to an A/G:C triple seen in the hammerhead crystal structure (Fig. 1d,f in Pley et al., 1994). The type of nucleotide quadruple shown in **D** has been observed in the hammerhead crystal structure and in the P4/P6 domain structure of the *Tetrahymena* ribozyme (Cate et al., 1996). Highlighted hydrogen bonding contacts in **B**, **C**, **D,** and **E** are supported by the interference results shown in **A**.

et al., 1995a). These findings have been considered in the Easterwood and Harvey model, where the N1 imino and O6 functions of G259 form H bonds with the N7 and the 6-NH_2 group of A_{76} (Fig. 7). In the NMR structure of a 31-meric RNA module mimicking the P15/16 region of *E. coli* RNase P RNA, the upper- and lower-loop nucleotides (corresponding to nt 254–259 and 291–295 in RNase P RNA; Fig. 3) were found to form a

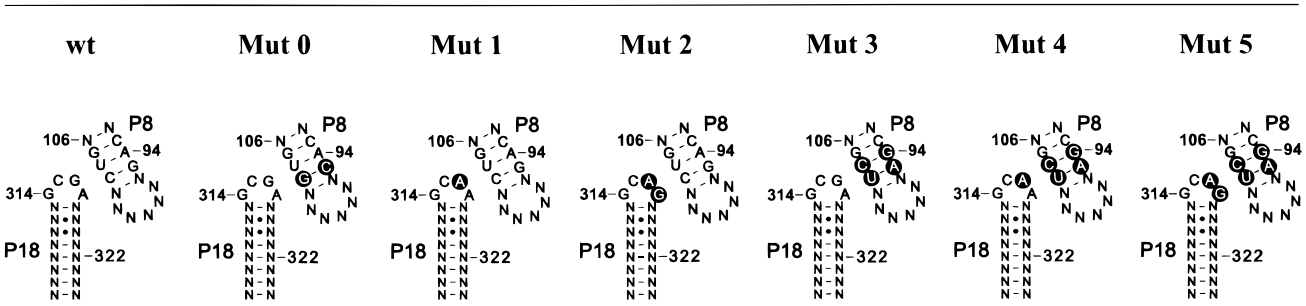

appK_D						
3.6 ± 0.8 nM	10.8 ± 2.1 nM	9.3 ± 3.4 nM	> 8 µM	201 ± 33 nM	107 ± 34 nM	> 8 µM
				Ca^{2+}, ptRNA		
				131 ± 27 nM	83 ± 27 nM	

FIGURE 5. Apparent equilibrium dissociation constants (appK_D) for tRNA binding to *E. coli* RNase P RNA variants with mutations in the P8 and/or L18 regions. Mutations in L18 and P8 are highlighted. AppK_D-values were measured by gel retardation in 1 × buffer A (see Materials and Methods) using trace amounts of radiolabeled $tRNA^{Gly}_{(intron)}$. For RNase P RNA variants Mut 3 and Mut 4 we also measured binding of substrate $ptRNA^{Gly}$ (appK_D-values given below the ones for $tRNA^{Gly}_{(intron)}$); however, in these two cases, Ca^{2+} was substituted for Mg^{2+} and the pH was reduced from 7.0 to 6.0 to avoid processing of ptRNA during preincubation and electrophoresis (for details, see Materials and Methods).

partial continuity of the base-stacked A-type RNA helices on both sides of this internal loop (Glemarec et al., 1996). NOE data also suggested that the nucleotide corresponding to G259 is exceptional in that it is in a bulged-out conformation (Glemarec et al., 1996). In addition, G259 lies within a prominent metal ion cleavage site whose susceptibility to lead hydrolysis is reduced in the presence of tRNA (Ciesiolka et al., 1994), and a G259-to-U modification changes cleavage site selection with some substrates in the presence of Mg^{2+} (Kufel & Kirsebom, 1996b). It should also be noted that the above-mentioned 31-meric RNA mimic of the J15/16 internal loop, which folds in a similar manner in the isolated state as within the RNase P RNA context, is an autonomous binding site for divalent metal ions that are critical for the interaction of this region with (p)tRNA ligands (Kufel & Kirsebom, 1998). Based on the observations just outlined it is likely that Rp-phosphorothioate-specific interference effects observed 5′ of guanosines 259–262 (Table 1) reflect indirect effects on tRNA binding by means of perturbing the P15/16 region and/or its interaction with metal ions.

Since gel-resolvable tRNA-binding to RNase P RNA substantially relies on the NCCA interaction (Hardt et al., 1995a), our interference assay seems to be highly sensitive to minor destabilizations in the P15/16 domain. Our observation of 2′-deoxy modifications at C253 and A256 that interfere with tRNA binding (Hardt et al., 1996) may also reflect a direct or indirect role of the 2′-hydroxyls at these positions in metal ion coordination or in stabilizing tertiary contacts between nucleotides in the J15/16 internal loop and other regions of RNase P RNA. In summary, it has become clear that the structural integrity of the J15/16 loop is tightly linked to its metal-ion binding properties and to the alignment of the cleavage site (Kufel & Kirsebom, 1996b; Westhof et al., 1996). The NCCA interaction seems to induce a structural rearrangement of the RNase P RNA-(p)tRNA complex including a recoordination of metal ion(s) in the vicinity of the cleavage site (Ciesiolka et al., 1994; Kufel & Kirsebom, 1996b; Westhof et al., 1996; Oh et al., 1998). Base, ribose, and phosphate moieties of nucleotides in the upper and lower parts of the J15/16 loop as well as base and ribose moieties of the tRNA NCCA terminus influence this process (Perreault & Altman, 1992; Hardt et al., 1996; Kufel & Kirsebom, 1996b, 1998; Tallsjö et al., 1996; Oh et al., 1998).

Combined Rp-phosphorothioate and inosine interference effects were observed at G250 and G300 (Table 1). The Rp-GMPαS interference at the phylogenetically conserved G300 is enhanced by additional inosine (Table 1) or 2′-deoxy modifications (Hardt et al., 1996). A G300-to-C mutation largely decreased tRNA binding affinity to *E. coli* RNase P RNA, although binding affinity could be partially restored at high monovalent salt concentrations. The G300-to-C mutation also caused differences in the susceptibility to lead hydrolysis in the J5/15 to P17 region (Hardt & Hartmann, 1996). In summary, G300 is critical for (p)tRNA binding and several functional groups of this nucleotide seem to be involved in an intricate, yet uncharacterized, network of interactions. Considering the just-mentioned

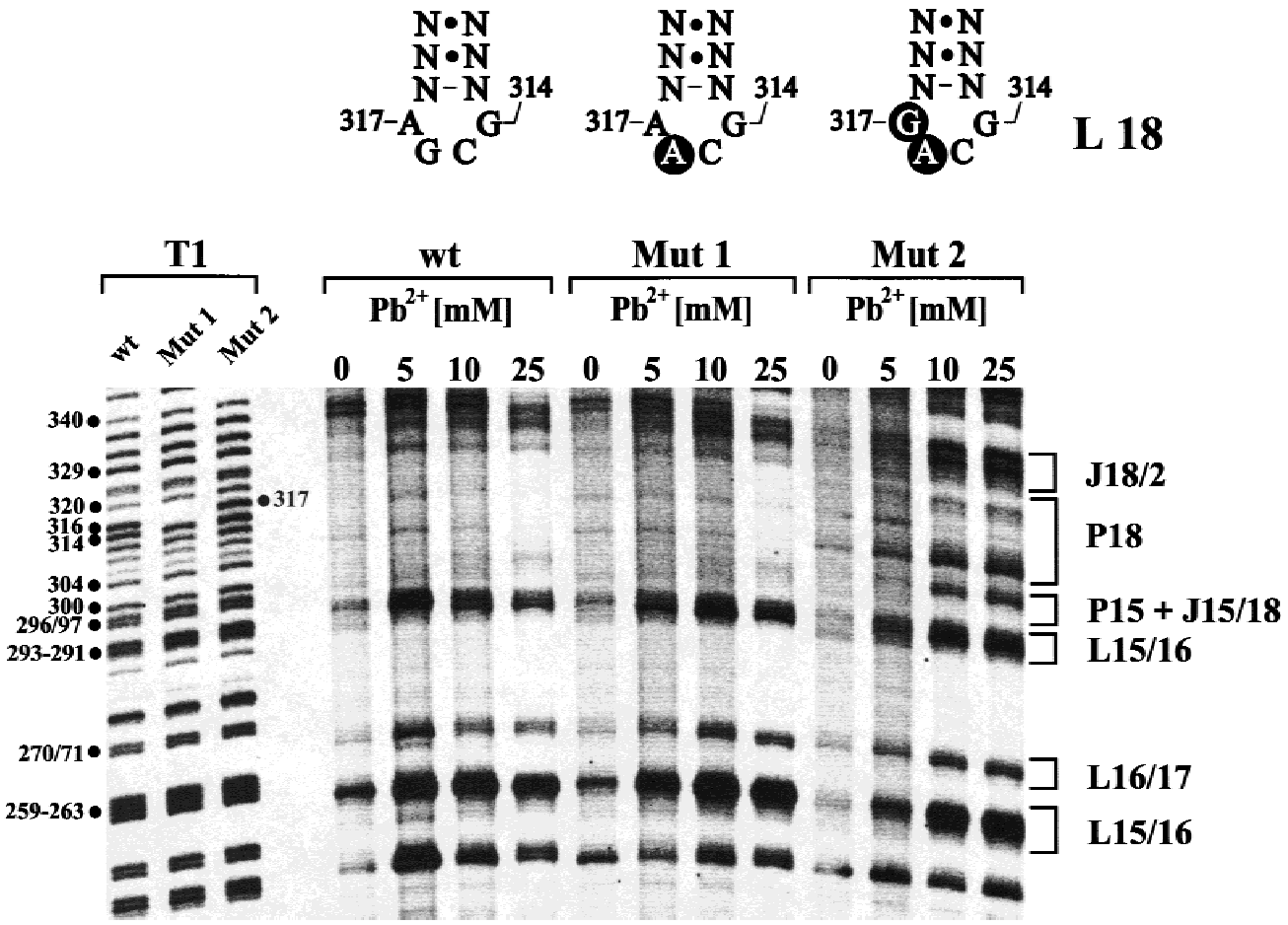

FIGURE 6. Pb^{2+}-induced hydrolysis patterns of 5′-^{32}P-labeled wild-type (wt) and mutant RNase P RNAs (Mut 1 and Mut 2). Sequence variations in the L18 tetraloop are shown at the top. Lanes T1: limited digestion with RNase T1; note that G316 is missing in RNAs Mut 1 and Mut 2, and a new G band appears at position 317 in RNA Mut 2. Assignment of Pb^{2+}-hydrolysis bands to secondary structural elements is given on the right (see also Zito et al., 1993; Ciesiolka et al., 1994). For details of the Pb^{2+}-hydrolysis assay, see Materials and Methods.

phenotype of the G300-to-C mutant, the universal conservation of G300 among bacterial and archaeal RNase P RNAs (RNase P database; Brown, 1998), and taking into account the two available models of the RNase P RNA-(p)tRNA complex (Chen et al., 1998; Massire et al., 1998), it is likely that G300 affects (p)tRNA binding indirectly by playing a crucial role in folding of the core structure, rather than forming a direct contact to the tRNA moiety.

Phylogenetic comparative analysis predicts that G250 forms a G-U pair with U299 in *E. coli* RNase P RNA. G250 is part of the core structure and several cross-links with (p)tRNAs carrying a photoreactive group near the tRNA 5′-end map to the preceding nucleotides A248/249 (Burgin & Pace, 1990; Kufel & Kirsebom, 1996a). This included ptRNAs carrying photoreactive 4-thio-U residues 1 nt upstream of the RNase P cleavage site (Kufel & Kirsebom, 1996a). As for G300, we think it likely that Rp-phosphorothioate and inosine modifications at G250 affect tRNA binding indirectly by perturbing folding of the RNase P RNA core structure.

Tertiary contacts L18/P8 and L14/P8

We present here, for the first time, two lines of experimental evidence—modification interference and a restoration of (p)tRNA binding affinity by compensatory mutations—in support of the L18/P8 tertiary contact. Evidently, the integrity of the L18/P8 is crucial for high affinity binding of the tRNA moiety. We propose here that the L18/P8 contact includes the formation of a nucleotide quadruple, as shown in Figure 4D, for the following reasons: (a) this type of quadruple has, up to now, been observed for two GNRA tetraloop-helix interactions in crystal structures (Pley et al., 1994; Cate et al., 1996), and (b) five sites of tRNA binding interference are in line with its formation (Fig. 4A). The proposed model for the adjacent G316/A94:U104 triple (Fig. 4E), although without crystallographic precedent, would best accommodate the observed modifications that interfere with tRNA binding. However, at present we cannot rule out that the L18/P8 tertiary contact involves interactions of the kind shown in Figure 4B,C

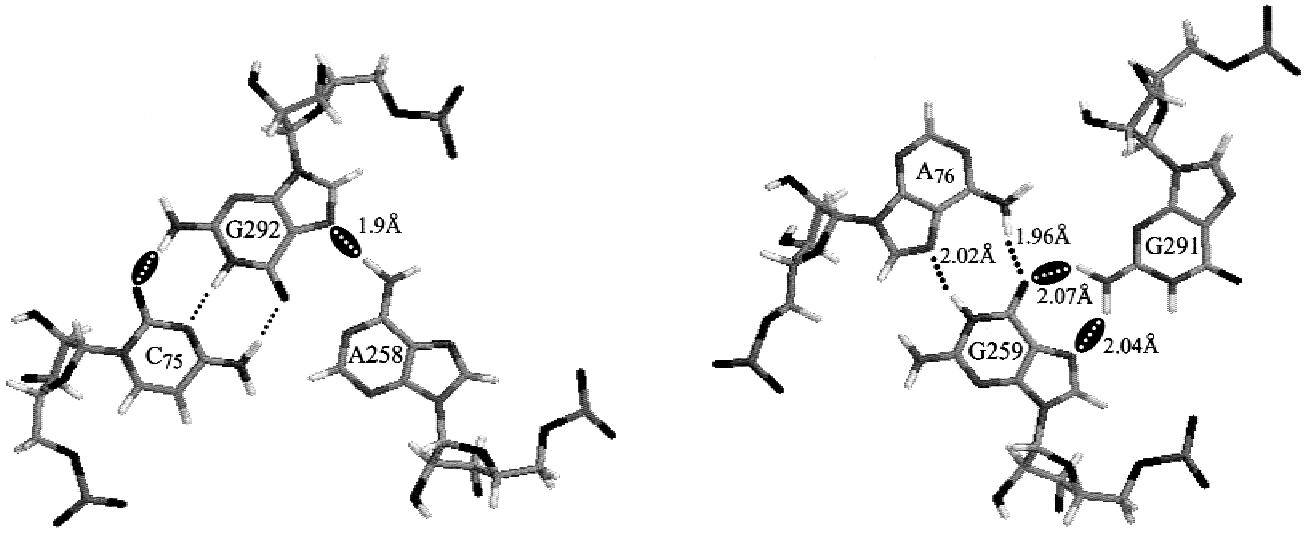

FIGURE 7. Model of consecutive base triples formed between C_{75} and A_{76} of tRNA 3′-CCA termini and nt G292/A258 and G291/G259 in loop 15 of *E. coli* RNase P RNA, as proposed by Easterwood & Harvey (1997). Highlighted hydrogen-bonding contacts are supported by the observed inosine interferences at G291 and G292 (Fig. 2A, Table 1) and by a c7-deaza interference at G292 (unpubl. result).

or may include hydrogen bonding contacts neither considered in Figure 4B,C nor in Figure 4D,E.

The phylogenetic covariation analysis of Brown et al. (1996) also suggested that A214 of *E. coli* RNase P RNA forms a triple with the base pair C93:G105 in P8. This tertiary interaction may include another triple formed between A215 and C92:G106 at the base of P8. We have observed inosine interference effects in the region of G105–109 (Table 1), which could not be assigned to individual guanosines because of poor gel resolution. Provided that inosine interferences at G105–109 included contributions of G105 and/or G106, our results might be interpreted in support of the L14/P8 interaction.

The J11/12 and J14/11 regions

Two sites of inosine interference were observed in the upper domain of *E. coli* RNase P RNA, namely at G137 and G230 (Table 1). G137 is in the vicinity of A130 and A132, where Rp-phosphorothioate modifications impair tRNA binding (Hardt et al., 1995b), and next to A136, where a 2′-deoxy modification interferes with tRNA binding (Hardt et al., 1996). Westhof et al. (1996) have proposed J11/12 to be an important contact site for tRNA substrates, which is consistent with the accessibility of nt 119–138 to oligonucleotide binding (Guerrier-Takada & Altman, 1993). The J11/12 region is much more accessible to Fe(II)-EDTA cleavage at 10 mM compared with 100 mM Mg^{2+}, demonstrating the crucial role of Mg^{2+} in organizing the higher-order structure of this region (Westhof et al., 1996). In the three-dimensional model of Massire et al. (1998), nt 136/137 are in proximity of the substrate-RNase P RNA interface, with the closest distance (4.2 Å) being from the 6-NH_2 group of A136 to the O-2P function of C56 of their tRNA. In this model, which, of course, does not claim to represent a high-resolution structure, neither the 2′-OH group of A136 nor the 2-NH_2 function of G137 would be in H-bonding distance to functional groups of the tRNA moiety. Thus, it remains unclear whether modifications at A136/G137 disrupt direct contacts to the tRNA moiety or affect tRNA binding indirectly by perturbing local RNase P RNA structure.

G230 was shown to pair with C128 by covariation and mutational analyses (Mattsson et al., 1994). According to a recent phylogenetic comparative analysis, the 230:128 bp could be in the center of a P11 helix extension, further involving non-Watson–Crick pairs at positions 129:229 and 127:231 (Massire et al., 1998). Inosine replacement at nt 230 may weaken this irregular P11 extension or may disrupt a tertiary interaction involving the 2-NH_2 group of G230. This may in turn destabilize the A233 contact with the tRNA T stem (Pan et al., 1995). A disruption of this contact may also be the consequence of a 2′-deoxy modification at A129 and Rp-phosphorothioate modifications 5′ of A130 and A132, all of which were found to impair tRNA binding (Hardt et al., 1995b, 1996).

The P11-J11/12-J14/11 regions play a key role in the interaction of RNase P RNA with metal ions: (a) the most prominent sites of lead hydrolysis have been assigned to C122/C123 and G137/C138 (Zito et al., 1993; Ciesiolka et al., 1994), and hydrolysis at these locations was also observed with other metal ions (Kazakov & Altman, 1991), (b) a G230-to-C mutation reduced

the rate of lead-induced hydrolysis at positions G137/C138 and in the J14/11 region (Mattsson et al., 1994), (c) impaired tRNA binding because of Rp-phosphorothioate modifications 5′ of A130 and A132 could be partially rescued by addition of Mn^{2+} (Hardt et al., 1995b), (d) the J11/12 and J14/11 regions appear rather unstructured at low- versus high-Mg^{2+} concentrations (Westhof et al., 1996), and (e) the region in yeast nuclear RNase P RNA corresponding to J11/12 was shown to affect Mg^{2+} utilization of the enzyme in vivo (Pagan-Ramos et al., 1996) and to form a structure that is highly sensitive to changes in the Mg^{2+}-concentration (Ziehler et al., 1998). It is thus conceivable that modifications in J11/12, such as the 2′-deoxy and inosine modifications at A136 and G137, shift the equilibrium to less productive conformations in the upper RNase P RNA domain, rather than reflecting direct contacts to the tRNA moiety. The finding of several modifications in the J11/12 region that interfere with tRNA binding (this study; Hardt et al., 1995b, 1996) as well as the clustered conservation of several nucleotides in J11/12 (Haas et al., 1994) supports the notion that this region folds into a complex, yet poorly understood structure.

The P2/P3, J3/4, P4 regions

Sites of inosine interference were observed at G19, linking P2 and P3, at G22 and G30 (P3) at G63/64 (J3/4), at G356 (P4), and a combined inosine/Rp-phosphorothioate effect at G72 in P4 (Table 1). All positions are remote from functional groups of the tRNA moiety in both existing models (Chen et al., 1998; Massire et al., 1998). Thus, inosine interference effects observed at these positions are less likely to reflect direct contacts. Based on Fe(II)-EDTA cleavage experiments, Westhof et al. (1996) have argued that some regions of *E. coli* RNase P RNA are conformationally more flexible than others, such as the internal G22/G59 loop in P3, and the region of about nt 40–75, which depends on high Mg^{2+} concentrations to adopt a more ordered structure. Thus, the absence of the 2-NH_2 group at G19, 22, 30, 63, 64, or 72 may alter the conformational equilibrium in these regions, which is then expected to affect the folding of structural elements that are in contact with the tRNA moiety. This may also explain the numerous interference effects identified in the core helix P4 and its flanking sequences in previous studies (Hardt et al., 1995b, 1996; Harris & Pace, 1995).

It is interesting to note that G19, 63, 64, and 356 are invariant among bacterial RNase P RNAs. G19 connects P2 and P3, which are stacked in the models of Massire et al. (1998) and Chen et al. (1998). G19 may function as an anchored hinge influencing the relative orientation of P2 and P3. Removal of its 2-NH_2 may disrupt a contact to unknown functional group(s) leading to rearrangements of the P2/P3 stack. Helix P4 is a universally conserved structural element of all RNase P and RNase MRP RNAs (Forster & Altman, 1990b; Schmitt et al., 1993), which is embedded in the tightly packed core structure (Chen et al., 1998; Massire et al., 1998) and known to interact with metal ions (Hardt et al., 1995b; Harris & Pace, 1995). Thus, 2-NH_2 groups of the identified invariant guanosines in P4 and J3/4 (G63, 64, and 356) are thought to be part of a hydrogen-bonding network required to organize the higher-order structure and the metal binding sites in the catalytic core, rather than being involved in direct contacts to tRNA moieties. Massire et al. (1998) have recently proposed that the two adenines 98/99 in L8 interact with the two conserved base pairs C71:G356 and C70:G357 in P4. In their model, N1 of A99 is at a distance of 3.5 Å to the 2-NH_2 group of G356, and N3 of A99 is 3.4 Å from the 2′-hydroxyl of C71. Our findings of an inosine interference at G356 (this study) and 2′-deoxy interferences at A99 and C71 (Hardt et al., 1996) provide the first direct experimental evidence in support of the formation of an A99/C71:G356 triple. Likewise, Rp-phosphorothioate modifications 5′ of C70 and C71 that also interfere with tRNA binding (Hardt et al., 1995b) and catalysis (Kazantsev & Pace, 1998) could as well reflect a perturbation of the proposed L8/P4 tertiary contact. We propose that the nucleotide triple A99/C71:G356 is of the kind observed in the hammerhead crystal (Fig. 1d of Pley et al., 1994), involving the following features: hydrogen bonding between N1 of A99 and the 2-NH_2 group of G356, between N3 of A99 and the 2′-hydroxyl of C71, and between the 2′-hydroxyls of C71 and A99 (Fig. 8). Clustered Rp-phosphorothioate

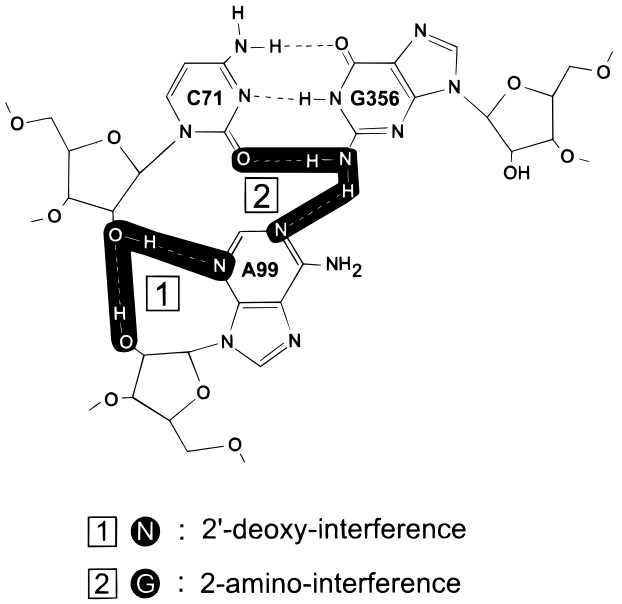

FIGURE 8. Model of a nucleoside triple formed between A99 in L8 and base pair C71:G356 (P4) of *E. coli* RNase P RNA (adapted from Pley et al., 1994). Highlighted hydrogen-bonding contacts are supported by our tRNA binding interference data (Table 1; Hardt et al., 1996; for details, see text).

modifications interfering with catalysis and tRNA binding have been observed in helix P4 (Hardt et al., 1995b; Harris & Pace, 1995; Kazantsev & Pace, 1998). The finding that interferences at A67, U69, and C70 were responsive to rescue by Mn^{2+} (Hardt et al., 1995b; Harris & Pace, 1995) as well as the critical role of the base at position 70 in determining the catalytic metal specificity (Frank & Pace, 1997) suggest that the putative L8-P4 contact is in direct proximity to metal-ion binding site(s).

Considering that the majority of guanosines in *E. coli* RNase P RNA is involved in Watson–Crick pairing and leaving aside the unresolved clusters G105–109 and G259–262, relatively few inosine interference effects were observed in regular helical segments (Fig. 3). Based on the involvement of G95 and G356 in the L18/P8 and L8/P4 tertiary interactions, it seems likely, by inference, that those other guanosines in regular helices showing inosine interference function as minor groove hydrogen bonding donors as well.

MATERIALS and METHODS

PCR, mutagenesis, and cloning

Primer 1: 5′-**TAATACGACTCACTATA**GGAAGCTGACCAG ACAGTCGCCGC
Primer 2: 5′-CCAGAATTCGAAAT**TAATACGACTCACTATA**
Primer 3: 5′-CGCGGATCC**A**GGTGAAACTGACCGATAAGC CGG
Primer 4: 5′-GTCCCCCGGGTAGGCTGCTTGAGCCAG
Primer 5: 5′-TATTACGTTTCGTCCTCACGGACTCATCAGA CCGGAAAGCACATCCGGTGA**C**GTGAAACTGACCGAT AAGCCGGGTTC
Primer 6: 5′-GGCGGGATCCTATTACGTTTCGTCCTCACGG ACTC
Primer 7: 5′-ACGCGTTACGTGGCACCCTGCCCTATG
Primer 8: 5′-CCATAGGGCAGGGTGCCACGTCCACGTAAC GCGTGG.

All PCR reactions were performed with Pfu DNA polymerase according to protocols provided by the manufacturer (Stratagene). The *E.coli* RNase P RNA wild-type gene (*rnpB*) was amplified using forward primer 1 (T7 promoter sequence in bold, nt 1 of RNase P RNA underlined, according to Fig. 3) and reverse primer 3 (*Bam*H1 site underlined, the nucleotide complementary to U377 of RNase P RNA in bold) and template pDW160 (Waugh & Pace, 1990) in a first PCR reaction, and using the resulting PCR product, forward primer 2 (*Eco*RI site underlined, T7 promoter in bold) and reverse primer 3 in a second reaction. The latter PCR product was digested with *Eco*RI and *Bam*HI and cloned into pSP64 (Promega) digested with the same enzymes, resulting in plasmid pSP64M1. Introduction of a *cis*-hammerhead-coding sequence adjacent to the 3′ end of *rnpB* was performed as follows: (1) amplification using forward primer 4 (*Sma*I site underlined, nt 288–293 in Fig. 3), reverse primer 5 (hammerhead sequence underlined, mutation at position 376 to generate a GUC sequence for optimized hammerhead cleavage in bold), and pSP64M1 as template; (2) a *Bam*HI site was introduced using forward primer 4 and reverse primer 6 (*Bam*HI site underlined); this PCR product was digested with *Sma*I and *Bam*HI and substituted for the corresponding *Sma*I/*Bam*HI fragment encoding the 3′-portion of *rnpB* in pSP64M1, yielding plasmid pSP64M1HH. Mutations in P8 (C95:G103) were introduced by a three-reaction PCR protocol as described previously (Hardt & Hartmann, 1996), using (a) primers 1 and 7 (mutations underlined, complementary to nt 78–104 in Fig. 3) and pSP64M1 as template in the first step, (b) primer 8 (mutations underlined, corresponding to nt 77–106 in Fig. 3), primer 3, and the template pSP64M1 in a second reaction, and (c) primers 1 and 3 and the two PCR products from the preceding steps as template DNAs in a third reaction. The final PCR product was blunt-end cloned into the *Sma*I site of pUC18. *E. coli* RNase P RNAs Mut 1–4 were constructed by site-directed mutagenesis using the method of Kunkel (1985) on single-stranded DNA obtained from a derivative of pDW98 (Smith et al., 1992) that contained an f1 origin of replication. Primers used are minus-strand oligonucleotides listed below. Mutagenic primers were used singly or in pairs to obtain the desired mutations; primer Ec316A: 5′-TAGGCCAGCAATTG CTCACTG (mutation underlined, complementary to nt 308–328 in Fig. 3); primer Ec316–317: 5′-TAGGCCAGCAA CTGCTCACTG (mutation underlined, complementary to nt 308–328 in Fig. 3); primer Ecp8-18d: 5′-TTCCCCCCC GAGCGTTACTCGGCACCCTG (mutations underlined, complementary to nt 85–113 in Fig. 3). Cloned PCR products and mutated *rnpB* genes were confirmed by DNA sequencing using Sequenase (US Biochemicals) or the ABI Prism Kit (Applied Biosystems).

Preparation of RNAs

Templates prepared by PCR were used for T7 transcription of wild-type *E. coli* RNase P RNA without a hammerhead, (p)$tRNA^{Gly}$ and (p)$tRNA^{Gly}_{(intron)}$ (Hardt et al., 1993b). Templates for all other RNAs were linearized plasmid DNAs. Unmodified *E. coli* RNase P RNA, (p)$tRNA^{Gly}$ and (p)$tRNA^{Gly}_{(intron)}$ were synthesized by runoff transcription with T7 RNA polymerase under the following conditions (1 mL assay): 80 mM HEPES/HCl, pH 7.5, 22 mM $MgCl_2$, 1 mM spermidine, 3.75 mM each ATP, CTP, GTP, and UTP, 120 μg BSA, 5 mM DTT, 5 U pyrophosphatase, about 15 pmol (linearized plasmid DNA) or 300 pmol (PCR-amplified DNA) template DNA and 2,000 U T7 RNA polymerase (MBI Fermentas). For the synthesis of RNAs with 5′-monophosphate or 5′-OH groups (to facilitate 5′-end labeling), T7 transcription assays contained either 9 mM GMP or 6 mM ApG as the initiator of transcription. Initiation with ApG introduced an additional A residue at the 5′ end, resulting, for example, in a $ptRNA^{Gly}$ with a 15-nt 5′ flank (5′-AGGAUUUUCCCUUUC). After 2 h at 37 °C, 250 U DNase I (Boehringer Mannheim) were added, followed by another incubation for 30 min at 37 °C and phenol/chloroform (1:1) extraction. RNAs were purified by Sephadex-G50 gel filtration and recovered by ethanol precipitation in the presence of 75 mM NaOAc, pH 6.7. RNAs were dissolved in water and concentrations were determined by absorbance at 260 nm (1 A_{260} unit = 37 μg). For the synthesis of phosphorothioate-modified RNase P RNAs, GTP was partially replaced with the Sp-GTPαS or Sp-ITPαS (NAPS Göttingen, Germany) analog. Partially Rp-inosine-phosphorothioate- (Rp-IMPαS) mod-

ified *E.coli* RNase P RNAs were prepared by T7 transcription in the presence of 40 mM Tris/HCl, pH 8.0, 2 mM NaCl, 8 mM $MgCl_2$, 2 mM spermidine, 5 mM DTT, 1 mM GTP, 1.5 mM each ATP, CTP, and UTP, 0.025 mM ITPαS, ~15 pmol (linearized plasmid DNA) or 300 pmol (PCR-amplified DNA) template DNA and 2,000 U T7 RNA polymerase. After digestion with DNase I, transcription assays were purified as described above.

3′- and 5′-end labeling

End labeling was performed essentially as reported previously (Hardt et al., 1995b). Labeled RNAs were purified by 5 to 10% PAGE/8 M urea, bands were visualized by autoradiography, excised from the gel, eluted overnight at 4 °C in 200 mM Tris/HCl, pH 7.1, 1 mM EDTA, 0.1% SDS, and were recovered by ethanol precipitation in the presence of 75 mM NaOAc (pH 6.7) and 13 μg/mL glycogen as carrier. Samples were dissolved in 10 μL water and stored at −20 °C. Before 3′-end labeling of RNase P RNA transcribed from plasmid pSP64M1HH and carrying the 3′ end U_{370}UUCACGUC>p derived from hammerhead self-cleavage, the 2′, 3′-cyclic phosphate was removed essentially as described (Cameron & Uhlenbeck, 1977). Reaction mixtures, containing 0.1 mM ATP, 100 mM imidazole-HCl, pH 6.0, 10 mM $MgCl_2$, 10 mM 2-mercaptoethanol, 20 μg/mL BSA, and 1 U T4 polynucleotide kinase (MBI Fermentas) per 86 pmol of RNA, were incubated for 6 h at 37 °C, followed by phenol/chloroform (1:1) and chloroform extractions, desalting on Sephadex G-50 columns, ethanol precipitation in the presence of 75 mM NaOAc, pH 6.7, and dissolving the RNA in water.

Gel retardation

To analyze $tRNA^{Gly}_{(intron)}$ binding to partially phosphorothioate-modified *E. coli* RNase P RNA pools, 1.2 μM unlabeled wild-type RNase P RNA mixed with trace amounts of ^{32}P-labeled pool RNA were preincubated at 37 °C for 60 min in 1 × buffer A [100 mM $Mg(OAc)_2$, 100 mM NH_4OAc, 1 mM EDTA, 50 mM TrisOAc, pH 7.0, at 37 °C]; 1.9 μM $ptRNA^{Gly}_{(intron)}$ in 1 × buffer A containing glycerol was added (final volume 15 μL, final glycerol concentration 5%); and assays were incubated for 30 min at 37 °C, resulting in complete maturation of the $ptRNA^{Gly}_{(intron)}$. Samples were loaded on a native 7.5% polyacrylamide gel and run for 12 h at 37 °C. The running buffer (1 × buffer A) was exchanged several times to ensure constant conditions during electrophoresis. The bound and unbound RNAs were visualized by autoradiography; bands were excised and polymerized into a 7% PAA/8 M urea gel followed by electrophoresis under 1 × TBE conditions. After autoradiography, RNase P RNA bands were excised again, eluted, and precipitated as described above. Gel retardation assays with mutant *E. coli* RNase P RNAs were performed as outlined above, but using trace amounts of 5′-end labeled $tRNA^{Gly}_{(intron)}$ or $tRNA^{Gly}$ incubated with increasing concentrations of RNase P RNAs in 1 × buffer A. For binding studies with the 5′-end labeled substrate $ptRNA^{Gly}$, the incubation and electrophoresis buffer contained 100 mM $Ca(OAc)_2$, 100 mM NH_4OAc, 1 mM EDTA and 50 mM MES, pH 6.0, at 37 °C (plus 5% glycerol in the incubation buffer) to prevent processing. The 5′-end label allowed us to ascertain that maturation of $ptRNA^{Gly}$ during the gel retardation procedure was insignificant.

Iodine hydrolysis

Iodine hydrolysis was performed as described (Hardt et al., 1995b). Hydrolysis bands were analyzed on 6, 8, 10, 15, or 25% PAA gels containing 8 M urea, and visualized and quantified using a Bio-Imaging Analyzer BAS-1000 (FUJIFILM) and the analysis software PCBAS (Raytest). Interference effects for individual bands were quantified as follows: $f_{nonbind.} = [I_{nonbind.}/(I_{nonbind.} + I_{complex})] \times 100\%$ and $f_{complex} = [I_{complex}/(I_{nonbind.} + I_{complex})] \times 100\%$, with $f_{nonbind.}$ and $f_{complex}$ indicating the fractional intensities of the nonbinding and binding (complex) RNase P RNA fractions, respectively. Intensities (I) were corrected for background values and $f_{complex}$ was normalized to the average intensities of three to four reference bands for which an interference effect was not apparent. For example, if the aforementioned three to four reference bands showed an average reduction in intensity by a factor of 0.9 in the lane corresponding to the RNase P RNA fraction from the complex, $f_{complex}$ was divided by this factor to avoid overemphasizing the interference effect. Finally, interference effects (in percent, Table 1) were determined by subtracting the corrected $f_{complex}$ value from the $f_{nonbind.}$ value.

Hydrolysis by Pb^{2+}

Trace amounts of 5′-^{32}P-labeled *E. coli* RNase P RNA and mutants thereof were mixed with 10 pmol of wild-type *E. coli* RNase P RNA and incubated for 1 h at 37 °C in 1.25 × buffer A. Pb^{2+}-hydrolysis reactions were started by adding 1 μL of lead acetate solution (25–125 mM) to 4 μL of RNA solution. In control lanes, 1 μL of water was added. After a 15 min incubation at 37 °C, hydrolysis reactions were stopped by addition of 10 μL loading buffer (67% formamide, 30 mM boric acid, 30 mM Tris/HCl, pH 8.3, 0.7 mM EDTA, 2.7 M urea, 0.01% [w/v] each BPB and XCB) supplemented with 75 mM EDTA and shock-freezing in liquid nitrogen.

RNA folding predictions and three-dimensional models

Folding predictions of *E. coli* RNase P RNAs with mutations in the P18 region were performed on the mfold web page (http://www.ibc.wustl.edu/~zuker/rna/form2.cgi). Computer models of RNase P RNA-(p)tRNA complexes (Chen et al., 1998; Massire et al., 1998) and the J15/16-ACCA interaction (Easterwood & Harvey, 1997) were extracted from the RNase P database (Brown, 1998) available on the internet (http://www.mbio.ncsu.edu/RNaseP/home.html) and visualized using the program RasMol, Windows Version 2.6.

ACKNOWLEDGMENTS

We thank James W. Brown for maintaining and updating the RNase P database, as well as Jürgen Baruth and Günter Schäfer for continuous support. We acknowledge Norman R. Pace, in whose laboratory the RNase P RNA mutant studies

were begun. This work was supported by the Deutsche Forschungsgemeinschaft (grant Ha 1672/7-1/7-2 to RKH).

Received August 24, 1998; returned for revision September 21, 1998; revised manuscript received September 30, 1998

REFERENCES

Brown JW. 1998. The ribonuclease P database. *Nucleic Acids Res 26*:351–352.

Brown JW, Nolan JM, Haas ES, Rubio MAT, Major F, Pace NR. 1996. Comparative analysis of ribonuclease RNase P RNA using gene sequences from natural microbial populations reveals tertiary structural elements. *Proc Natl Acad Sci USA 91*:3001–3006.

Burgin AB, Pace NR. 1990. Mapping the active site of ribonuclease RNase P RNA using a substrate containing a photoaffinity agent. *EMBO J 9*:4111–4118.

Cameron V, Uhlenbeck OC. 1977. 3′-phosphatase activity in T4 polynucleotide kinase. *Biochemistry 16*:5120–5126.

Carrara G, Calandra P, Fruscoloni P, Tocchini-Valentini GP. 1995. Two helices plus a linker: A small model substrate for eukaryotic RNase P. *Proc Natl Acad Sci USA 92*:2627–2631.

Cate JH, Gooding AR, Podell E, Zhou K, Golden BL, Kundrot CE, Cech TR, Doudna JA. 1996. Crystal structure of a group I ribozyme domain: Principles of RNA packing. *Science 273*:1678–1685.

Chen J-L, Nolan JM, Harris ME, Pace NR. 1998. Comparative photocrosslinking analysis of the tertiary structure of *Escherichia coli* and *Bacillus subtilis* RNase P RNAs. *EMBO J 17*:1515–1525.

Christian EL, Yarus M. 1992. Analysis of the role of phosphate oxygens in the group I intron from *Tetrahymena*. *J Mol Biol 228*:743–758.

Ciesiolka J, Hardt W-D, Schlegl J, Erdmann VA, Hartmann RK. 1994. Lead-ion induced cleavage of RNase P RNA. *Eur J Biochem 219*:49–56.

Easterwood TR, Harvey SC. 1997. Ribonuclease RNase P RNA: Models of the 15/16 bulge from *Escherichia coli* and the P15 stem loop of *Bacillus subtilis*. *RNA 3*:577–585.

Forster AC, Altman S. 1990a. External guide sequences for an RNA enzyme. *Science 249*:783–785.

Forster AC, Altman S. 1990b. Similar cage-shaped structures for the RNA components of all ribonuclease P and ribonuclease MRP enzymes. *Cell 62*:407–409.

Frank DN, Pace NR. 1997. In vitro selection for altered divalent metal specificity in the RNase P RNA. *Proc Natl Acad Sci USA 94*:14355–14360.

Gish G, Eckstein F. 1988. DNA and RNA sequence determination based on phosphorothioate chemistry. *Science 240*:1520–1522.

Glemarec C, Kufel J, Földesi A, Maltseva T, Sandström A, Kirsebom LA, Chattopadhyaya J. 1996. The NMR structure of 31mer domain of *Escherichia coli* RNase P RNA using its non-uniformly deuterium labelled counterpart [the "NMR-window" concept]. *Nucleic Acids Res 24*:2022–2035.

Guerrier-Takada C, Gardiner K, Marsh T, Pace N, Altman S. 1983. The RNA moiety of ribonuclease P is the catalytic subunit of the enzyme. *Cell 35*:849–857.

Guerrier-Takada C, Altman S. 1993. A physical assay for and kinetic analysis of the interactions between M1 RNA and tRNA precursor substrates. *Biochemistry 32*:7152–7161.

Haas ES, Banta AB, Harris JK, Pace NR, Brown JW. 1996. Structure and evolution of ribonuclease P RNA in Gram-positive bacteria. *Nucleic Acids Res 24*:4775–4782.

Haas ES, Brown JW, Pitulle C, Pace NR. 1994. Further perspective on the catalytic core and secondary structure of ribonuclease RNase P RNA. *Proc Natl Acad Sci USA 91*:2527–2531.

Hardt W-D, Erdmann VA, Hartmann RK. 1996. Rp-deoxy-phosphorothioate modification interference experiments identify 2′-OH groups in RNase P RNA that are crucial to tRNA binding. *RNA 2*:1189–1198.

Hardt W-D, Hartmann RK. 1996. Mutational analysis of the joining regions flanking helix P18 in *E. coli* RNase P RNA. *J Mol Biol 259*:422–433.

Hardt W-D, Schlegl J, Erdmann VA, Hartmann RK. 1993a. Role of the D arm and the anticodon arm in tRNA recognition by eubacterial and eukaryotic RNase P enzymes. *Biochemistry 32*:13046–13053.

Hardt W-D, Schlegl J, Erdmann VA, Hartmann RK. 1993b. Gel retardation analysis of *E. coli* M1 RNA-tRNA complexes. *Nucleic Acids Res 21*:3521–3527.

Hardt W-D, Schlegl J, Erdmann VA, Hartmann RK. 1995a. Kinetics and thermodynamics of the RNase P RNA cleavage reaction: Analysis of tRNA 3′-end variants. *J Mol Biol 247*:161–172.

Hardt W-D, Warnecke JM, Erdmann VA, Hartmann RK. 1995b. Rp-phosphorothioate modifications in RNase P RNA that interfere with tRNA binding. *EMBO J 14*:2935–2944.

Harris ME, Nolan JM, Malhotra A, Brown JW, Harvey SC, Pace NR. 1994. Use of photoaffinity crosslinking and molecular modeling to analyze the global architecture of ribonuclease RNase P RNA. *EMBO J 13*:3953–3963.

Harris ME, Pace NR. 1995. Identification of phosphates involved in catalysis by the ribozyme RNase P RNA. *RNA 1*:210–218.

Jaeger L, Michel F, Westhof E. 1994. Involvement of a GNRA tetraloop in long-range RNA tertiary interactions. *J Mol Biol 236*:1271–1276.

Kahle D, Wehmeyer U, Krupp G. 1990. Substrate recognition by RNase P and by the catalytic M1 RNA: Identification of possible contact points in pre-tRNAs. *EMBO J 9*:1929–1937.

Kazakov S, Altman S. 1991. Site-specific cleavage by metal ion cofactors and inhibitors of M1 RNA, the catalytic subunit of RNase P from *Escherichia coli*. *Proc Natl Acad Sci USA 88*:9193–9197.

Kazantsev AV, Pace NR. 1998. Identification by modification-interference of purine N-7 and ribose 2′-OH groups critical for catalysis by bacterial ribonuclease P. *RNA 4*:937–947.

Kirsebom LA, Svärd SG. 1994. Base pairing between *Escherichia coli* RNase P RNA and its substrate. *EMBO J 13*:4870–4876.

Kufel J, Kirsebom LA. 1996a. Different cleavage sites are aligned differently in the active site of M1 RNA, the catalytic subunit of *Escherichia coli* RNase P. *Proc Natl Acad Sci USA 93*:6085–6090.

Kufel J, Kirsebom LA. 1996b. Residues in *Escherichia coli* RNase P RNA important for cleavage site selection and divalent metal ion binding. *J Mol Biol 263*:685–698.

Kufel J, Kirsebom LA. 1998. The P15-loop of *Escherichia coli* RNase P RNA is an autonomous divalent metal ion binding domain. *RNA 4*:777–788.

Kunkel TA. 1985. Rapid and efficient site-specific mutagenesis without phenotypic selection. *Proc Natl Acad Sci USA 82*:488–492.

LaGrandeur TE, Hüttenhofer A, Noller HF, Pace NR. 1994. Phylogenetic comparative chemical footprint analysis of the interaction between ribonuclease RNase P RNA and tRNA. *EMBO J 13*:3945–3952.

Loria A, Pan T. 1997. Recognition of the T stem-loop of a pre-tRNA substrate by the ribozyme from *Bacillus subtilis* ribonuclease P. *Biochemistry 36*:6317–6325.

Massire C, Jaeger L, Westhof E. 1998. Derivation of the three-dimensional architecture of bacterial ribonuclease RNase P RNAs from comparative sequence analysis. *J Mol Biol 279*:773–793.

Mattsson JG, Svärd SG, Kirsebom LA. 1994. Characterization of the *Borrelia burgdorferi* RNase P RNA gene reveals a novel tertiary interaction. *J Mol Biol 241*:1–6.

McClain WH, Guerrier-Takada C, Altman S. 1987. Model substrates for an RNA enzyme. *Science 238*:527–530.

Nolan JM, Burke DM, Pace NR. 1993. Circularly permuted tRNAs as specific photoaffinity probes of ribonuclease RNase P RNA structure. *Science 261*:762–765.

Oh B-K, Frank DN, Pace NR. 1998. Participation of the 3′-CCA of tRNA in the binding of catalytic Mg^{2+} ions by ribonuclease P. *Biochemistry 37*:7277–7283.

Pagan-Ramos E, Lee Y, Engelke DR. 1996. A conserved RNA motif involved in divalent cation utilization by nuclear RNase P. *RNA 2*:1100–1109.

Pan T, Jakacka M. 1996. Multiple substrate binding sites in the ribozyme from *Bacillus subtilis* RNase P. *EMBO J 15*:2249–2255.

Pan T, Loria A, Zhong K. 1995. Probing of tertiary interactions in RNA: 2′-hydroxyl-base contacts between the RNase P RNA and pre-tRNA. *Proc Natl Acad Sci USA 92*:12510–12514.

Perreault J-P, Altman S. 1992. Important 2′-hydroxyl groups in model

substrates for M1 RNA, the catalytic RNA subunit of RNase P from *Escherichia coli*. *J Mol Biol 226*:399–409.
Pley HW, Flaherty KM, McKay DB. 1994. Model for an RNA tertiary interaction from the structure of an intermolecular complex between a GAAA tetraloop and an RNA helix. *Nature 372*:111–113.
Schlegl J, Fürste JP, Bald R, Erdmann VA, Hartmann RK. 1992. Cleavage efficiencies of model substrates for ribonuclease P from *Escherichia coli* and *Thermus thermophilus*. *Nucleic Acids Res 20*:5963–5970.
Schmitt ME, Bennett JL, Dairaghi DJ, Clayton DA. 1993. Secondary structure of RNase MRP RNA as predicted by phylogenetic comparison. *FASEB J 7*:208–213.
Smith D, Burgin A, Haas ES, Pace NR. 1992. Influence of metal ions on the ribonuclease P reaction. *J Biol Chem 267*:2429–2436.
Strobel SA, Shetty K. 1997. Defining the chemical groups essential for *Tetrahymena* group I intron function by nucleotide analog interference mapping. *Proc Natl Acad Sci USA 94*:2903–2908.
Svärd SG, Kagardt U, Kirsebom LA. 1996. Phylogenetic comparative mutational analysis of the base-pairing between RNase P RNA and its substrate. *RNA 2*:463–472.
Tallsjö A, Kufel J, Kirsebom LA. 1996. Interaction between *Escherichia coli* RNase P RNA and the discriminator base results in slow product release. *RNA 2*:299–307.
Thurlow DL, Shilowski D, Marsh TL. 1991. Nucleotides in precursor tRNAs that are required intact for catalysis by RNase P RNAs. *Nucleic Acids Res 19*:885–891.
Wang MJ, Davis NW, Gegenheimer P. 1988. Novel mechanisms for maturation of chloroplast transfer RNA precursors. *EMBO J 7*:1567–1574.
Waugh DS, Pace NR. 1990. Complementation of an RNase P RNA (*rnpB*) gene deletion in *Escherichia coli* by homologous genes from distantly related eubacteria. *J Bacteriol 172*:6316–6321.
Westhof E, Wesolowski D, Altman S. 1996. Mapping in three dimensions of regions in a catalytic RNA protected from attack by an Fe(II)-EDTA reagent. *J Mol Biol 258*:600–613.
Yuan Y, Altman S. 1995. Substrate recognition by human RNase P: Identification of small model substrates for the enzyme. *EMBO J 14*:159–168.
Ziehler WA, Yang J, Kurochkin AV, Sandusky PO, Zuiderweg ERP, Engelke DR. 1998. Structural analysis of the P10/11-P12 domain of yeast RNase P RNA and its interaction with magnesium. *Biochemistry 37*:3549–3557.
Zito K, Hüttenhofer A, Pace NR. 1993. Lead-catalyzed cleavage of ribonuclease P RNA as a probe for integrity of tertiary structure. *Nucleic Acids Res 21*:5916–5920.